CFD Validation and Verification of Airflow Characteristics in Indoor Swimming Pool

Ahmed M. Hanafi*, Mohamed A. Ibrahim

October 6 University, Faculty of Engineering, Mechatronics Engineering, 6th of October City, Giza, Egypt

Taher M. Abou-deif, Samy M. Morcos

Cairo University, Faculty Of Engineering, Mechanical Power Engineering, Cairo, Egypt

ABSTRACT

This research examines the impact of air curtain flows on heat and mass transfer within an indoor swimming pool facility, which plays a crucial role in providing both thermal comfort and hygiene. The study utilizes computational fluid dynamics (CFD) simulations, employing a commercial software package, ANSYS Fluent 17.2, to solve governing equations for energy, species transport, and turbulence closure through the k-epsilon model. A total of over 5.6 million mesh elements were used to generate comprehensive and accurate predictions of flow regimes. The geometry of a semi-Olympic pool located at Bishop's University in Sherbrooke, Quebec, Canada, with a coarsely trapezoidal shape and dimensions of 34.5 m x 25 m x 8 m, was modeled using SpaceClaim 3D software. The impact of the number and location of ventilation and air conditioning supply was also considered. Results were validated against OpenFOAM software, indicating good agreement. The research provides valuable insights into the effects of air curtain flows on indoor pool environments, which can inform the design and operation of air conditioning systems for indoor pools.

1. Introduction

Indoor swimming pools require efficient and reliable air conditioning systems, which not only maintain a comfortable climate but also ensure adequate dehumidification to prevent the buildup of moisture in the air. In many sports pools, large areas are dedicated not only to the pool itself but also to spectator seating and grandstands. The resulting high levels of water evaporation demand a well-designed and precisely controlled air conditioning system to operate continuously, regardless of the intensity of use of the pool hall. Indoor swimming pool air conditioning is a complex system, and its design must consider factors such as air distribution, thermal comfort, and hygiene to provide optimal conditions for users. Despite significant advances in air conditioning technology, the design and operation of such systems require careful consideration to ensure optimal performance. This study aims to investigate the effect of air curtain flows on heat and mass transfer in an indoor swimming pool hall, intending to improve our understanding of the complex interactions involved in designing and operating such systems.

1.1 Previous Researches

A. Limane et al. [1]: performed a simulation of the 3D airflow with mass and heat transfer in a complicated structure indoor swimming pool using the OpenFOAM software. The comparison of the airflow characteristics showed good agreement. Two simulations executed by summer and winter boundary conditions. Their comparison showed a minimal outcome on the inner situation which is displayed by a larger temperature difference in winter. Additionally, the effect of swimmers on the atmosphere evaluated and found to be of great importance.

The study showed that it is can simulate this 3D model airstream with mass and heat transfer by the software OpenFOAM code. Therefore, CFD simulation studies of the environments in big volumes with HVAC can perform at little prices. The numerical outcomes gained by changing the RANS turbulence models are suitable. But, the outcomes gained by the model k-e Launder & Sharma are the greatest acceptable.

M. M. Shah [2]: studied the approaches for an estimate of the evaporation rate of water vapor from water surfaces. The study presented and discussed the correlations between enclosing crowded and uncrowded water pools Including approaches offered for both types.

➢ Unoccupied swimming pool

➢ Use a larger mass flow rate between Equations 1 and 2

$$E_0 = C\rho_w(\rho_r - \rho_w)^{\frac{1}{3}}(W_w - W_r) \qquad (1)$$

$$E_0 = b(p_w - p_r) \qquad (2)$$

➢ Occupied swimming pool

$$\frac{E_{occ}}{E_0} = 1.9 - 21(\rho_r - \rho_w) + 5.3N^* \qquad (3)$$

$Where$:

✓ E_o = rate of evaporation from the occupied swimming pool, $\frac{kg}{m^2 \cdot h}$

✓ E_{occ} = $r$ate of evaporation from the occupied swimming pool $\frac{kg}{m^2 \cdot h}$

✓ p = $p$artial pressure of water vapor in the air, Pa

✓ W = specific humidity of the air, kg of $\frac{moisture}{kg}$ of air

✓ ρ = density of air, the mass of dry airper unit volume of moist air, $\frac{kg}{m^3}$

✓ r = at room temperature and humidity

✓ w = saturated at water surface temperature

✓ $N*$ is the number of occupants per unit pool area

✓ $C = 35$

✓ $b = 0.00005$

Mohamed Abo Elazm et al. [3]: Investigated the effect of air velocity, and evaporation rate on the indoor air quality in an enclosed swimming pools hall (San-Stefano Grand Plaza swimming pool which located in Alexandria, Egypt) has been carried out using CFD modeling. It was found from this study that the increase in the evaporation rate from the swimming pool surface is due to the lower temperature difference between air and water. The simulation results showed that the supply air velocity and temperature have a significant effect on the rate of evaporation, optimizing these two parameters could improve the indoor air quality inside enclosed swimming pools.On the other hand, increasing the supply air velocity resulted in a reduction in relative humidity and temperature which enhance the indoor air quality within enclosed swimming pools.
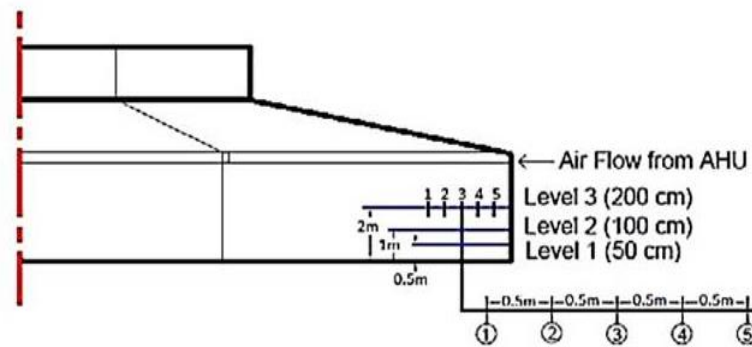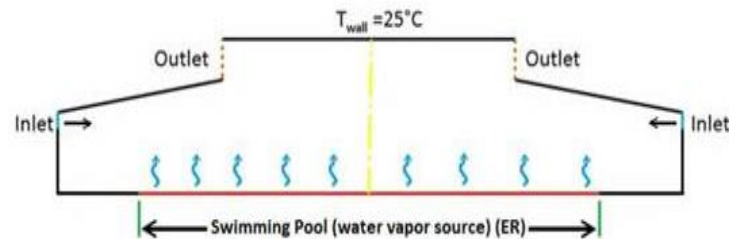
Figure 1: Thermocouples located at different levels [3]

Figure 2: Proposed 2D model for the indoor swimming pool [3]

1.2 Presented study

The numerical model investigation, incorporated in the present study, is used to investigate the airflow pattern, temperature, relative humidity distributions and the thermal comfort prediction based on the PMV model and the PPD model inside a semi-Olympic pool located at Bishop's University in Sherbrooke (Quebec, Canada).

Figure 3 : Inside a semi-Olympic pool located at Bishop's University in Sherbrooke

This study aims to validate the results of ANSYS Fluent with previous experimental and numerical work of A. Limane et al. [1]. The work of A. Limane et al. used to validate the numerical results with the experimental results by simulations of the 3D airflow using OpenFOAM software. The Present comparisons between the numerical results using ANSYS Fluent Software to those previously published experimental and numerical results obtained by different researchers in the field using OpenFOAM software.

1.2.1 Swimming Pool Description

The present validation concerns a semi-Olympic pool located at Bishop's University in Sherbrooke (Quebec, Canada). The space considered consists of a large enclosure with complex geometry, of roughly trapezoidal shape and dimensions of $(34.5 \text{ m} \times 25 \text{ m} \times 8 \text{ m})$. The

enclosure consists of the water basin area, and the spectator stands, the two major parts partially separated from each other as shown in Figure 4. It has two exterior partially subterranean walls (in contact with the external environment) located on the north and west sides and two interior walls located on the east and south sides.
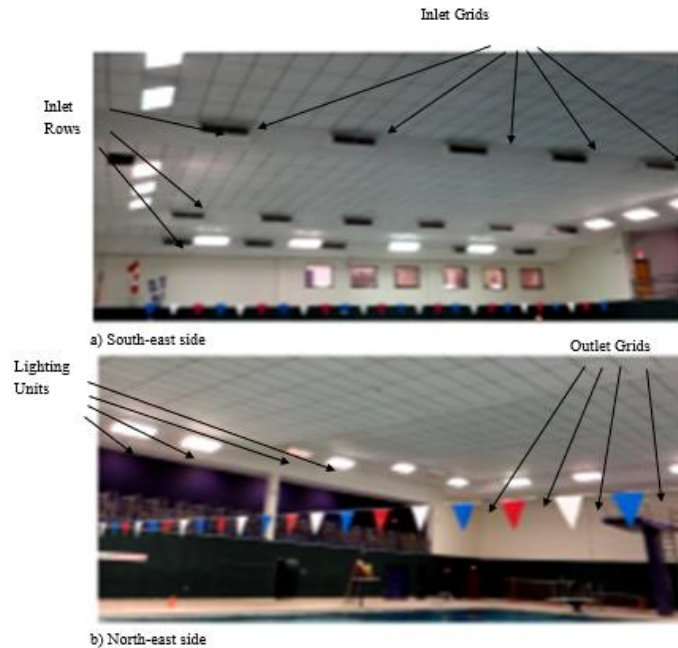

Figure 4: Inlet and outlet configuration [4]

The control of the air temperature in the pool is ensured exclusively by the HVAC system. The many inlets and outlets of the ventilation system create a complicated flow field. The water basin area: roofed on its inclined parts by a false ceiling with six horizontal segments at different heights a), scattered with three rows of air supply, each row with six air inlets ($1.05 \text{ m} \times 0.19 \text{ m}$) introducing air at an angle of $30°$ from horizontal. The air outlets ($1.20 \text{ m} \times 0.6 \text{ m}$) are all placed at the top of one horizontal segment on the opposite side (north side) to the three rows of air inlets. The spectator stands: covered with a long false ceiling and including six air inlets ($0.3 \, m \times 0.3 \, m$) which introduce the air on three sides at an angle of $30°$ from the horizontal.
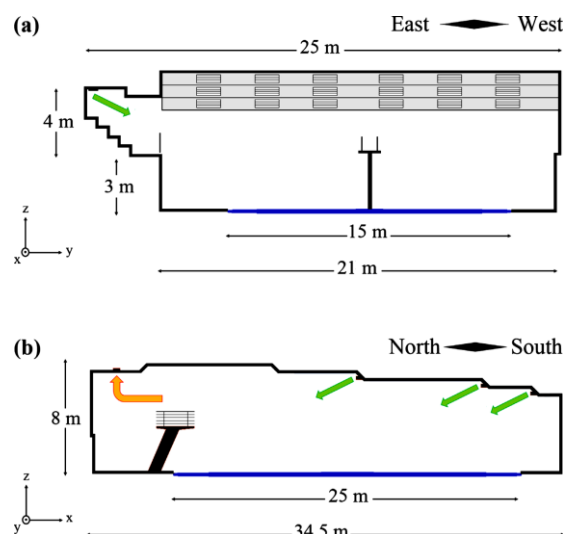

Figure 5: Pool dimensions and position of ventilation inlets/outlets:(a) Cross-section showing the position of spectator stands(b) Longitudinal section showing a form of a false ceiling (not to scale) [1]

2. Methods

CFD is a powerful tool for the analysis of fluid flows. It is a computer-based simulation technique providing an approximate two or three-dimensional solution to the equations governing fluid motion. The technique characterized by a division of the region in which flow is to be computed the computational domain, into a vast number of much smaller domains commonly referred to as mesh or grid cells. time-dependent flows and Complex geometries readily handled. The solution consists of values of flow parameters of interest such as velocity or gas concentration, calculated at each of the grid cells. [5] It provides a complete time-dependent picture of complex fluid flows. It works by solving the equations for the conservation of mass, momentum, turbulence, and energy at every cell over a region of interest with prescribed (known) conditions on the region boundary. Commonly known as the Navier-Stokes equation, these equations are highly non-linear partial differential equations that describe the fundamental behavior of the fluid. Because these equations cannot solve in a closed form, this CFD software employs what are known as "differencing" techniques to derive approximate solutions to the equations throughout the geometry modeled. CFD makes use of computer simulation to obtain an approximate solution of the governing equations of fluid flow [6].

For the present study, CFD simulation for airflow inside the swimming pool hall, numerical techniques were used to model the airflow characteristics. The governing equations in this model are Continuity, Momentum, and Energy equations [7] [8].

➢ Continuity equation with three-dimensional:

$$\frac{\partial \rho}{\partial t} + \frac{\partial(\rho u)}{\partial x} + \frac{\partial(\rho v)}{\partial y} + \frac{\partial(\rho w)}{\partial z} = 0$$

➢ Three momentum equations in Cartesian x, y, and z coordinates:

$$\rho \frac{Du}{Dt} = \rho g_x - \frac{\partial P}{\partial x} + \frac{\partial \tau_{xx}}{\partial x} + \frac{\partial \tau_{yx}}{\partial y} + \frac{\partial \tau_{zx}}{\partial z}$$

$$\rho \frac{Dv}{Dt} = \rho g_y - \frac{\partial P}{\partial y} + \frac{\partial \tau_{xy}}{\partial x} + \frac{\partial \tau_{yy}}{\partial y} + \frac{\partial \tau_{zy}}{\partial z}$$

$$\rho \frac{Dw}{Dt} = \rho g_z - \frac{\partial P}{\partial z} + \frac{\partial \tau_{xz}}{\partial x} + \frac{\partial \tau_{yz}}{\partial y} + \frac{\partial \tau_{zz}}{\partial z}$$

➢ Energy equation:

$$\rho \frac{\partial h}{\partial t} + \rho u \frac{\partial h}{\partial x} + \rho v \frac{\partial h}{\partial y} + \rho w \frac{\partial h}{\partial z} = \frac{\partial}{\partial x}\left[k \frac{\partial T}{\partial x}\right] + \frac{\partial}{\partial y}\left[k \frac{\partial T}{\partial y}\right] + \frac{\partial}{\partial z}\left[k \frac{\partial T}{\partial z}\right] + \emptyset$$

Where :

✓ $k = Thermal\ conductivity\ coefficient, W/m\ °C$
✓ $h = Enthalpy, kJ/kg$
✓ $\rho = Density, kg/m^3$
✓ $p = Pressure, Pa$
✓ $t = Time, s$
✓ $T = Dry\ bulb\ Temperature\ of\ gas\ mixture, K$
✓ $g = Gravitational\ acceleration, m/s^2$
✓ $x, y, z = Cardinal\ coordinate\ components$
✓ $u = Instantaneous\ velocity\ component\ in\ x\ direction, m/s$
✓ $v = Instantaneous\ velocity\ component\ in\ y\ direction, m/s$
✓ $w = Instantaneous\ velocity\ component\ in\ z\ direction, m/s$
✓ $\tau_{ij} = Subgrid-scale\ stress$

3. Numerical Validation

This study aims to validate the results of ANSYS Fluent with previous experimental and numerical work of A. Limane et al. [1]. The work of A. Limane et al. used to validate the numerical results with the experimental results by simulations of the 3D airflow using OpenFOAM software. The Present comparisons between the numerical results using ANSYS Fluent Software to those previously published experimental and numerical results obtained by different researchers in the field using OpenFOAM software.

3.1 Boundary Conditions:

The boundary conditions used in the present study for the indoor swimming pool were defined using a color-coded diagram, as shown in Figure 6. The inlet grille, outlet grille, and lighting unit were included in the diagram to accurately represent the geometry of the pool hall. Each color in the diagram corresponded to a specific boundary condition, with the blue color representing the Swimming pool, the red color representing the Outlet grille, and the green color representing the Inlet grille. The boundary conditions for each component were carefully selected and implemented to ensure accurate simulation results.
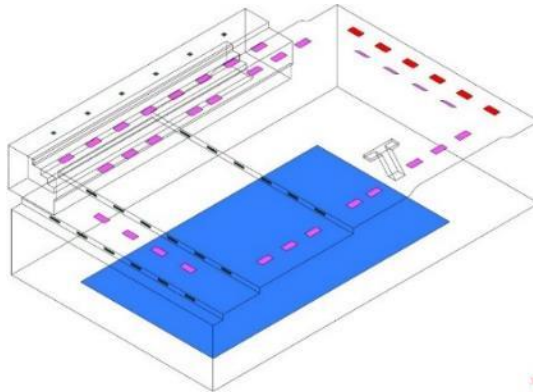
■ Swimming pool   ■ Inlet grille   ■ Outlet grille   ■ Lighting unit

Figure 6: Isometric view of the swimming pool hall
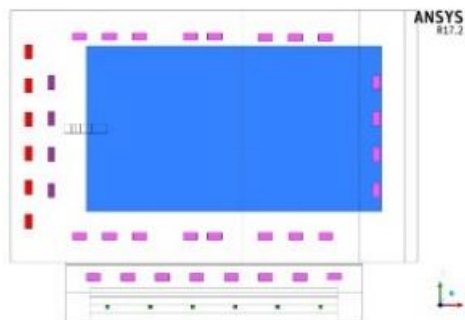

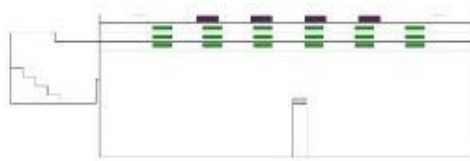**Figure 7: Plan view of the swimming pool hall**

Figure 8: Side view of the swimming pool hall

3.1.1 The Inlet Air Conditions:

In Table 1, the boundary conditions for the inlet of dimensions 1.05 m x 0.19 m are presented. The type of inlet condition used in the simulation was a velocity inlet, with a velocity of 3.5 m/s and an angle of 30º. The hydraulic diameter of the inlet was 0.3217 m, and the length of the inlet was set to 1.05 m. The temperature of the inlet air was set at 35 ℃, while the specific humidity was set to 0.017839 Kg/kg.

Furthermore, the component of the flow direction was defined, with values of X=-1, Y=0, and Z=-0.87. The length of the inlet in the flow direction was 0.2252 m. These boundary conditions were carefully selected to ensure accurate simulation results for the velocity, temperature, and humidity distribution within the swimming pool hall.

Table 1: Boundary conditions of the inlet $1.05\ m \times 0.19\ m$

Type	Velocity inlet	Hydraulic diameter	0.3217 m
Length	1.05 m	Temperature	35 ℃
Width	0.19 m	Specific humidity	0.017839 Kg/kg
Velocity	3.5 m/s	Angle	30º
Length	0.2252 m	Component of flow direction	$X = -1$ $Y = 0$ $Z = -0.87$

The spectator stands: roof with a long false ceiling and including six air supplies ($0.09\ m^2$) shown in Figure 9: Inlet which introduces the air on three sides, which introduces the air on three sides at an angle of 30° from the horizontal.
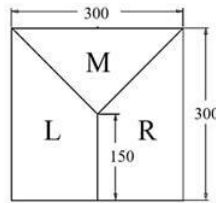

Figure 9: Inlet which introduces the air on three sides

Table 2: Boundary conditions of the inlet $30\ cm \times 30\ cm$

Inlet Side	R	L	M
Area	33750 mm^2	33750 mm^2	22500 mm^2
Perimeter	812.132 mm	812.132 mm	724.264 mm
Hydraulic Diameter	0.1662 m	0.1662 m	0.1242 m
Type	Velocity inlet		
Velocity	3.5 m/s		
Angle	30° from the horizontal.		
Component Of Flow Direction	$X = 1$ $Y = 0$ $Z = -0.87$	$X = -1$ $Y = 0$ $Z = -0.87$	$X = 0$ $Y = 1$ $Z = -0.87$
Temperature	35℃		
Specific Humidity	0.01784 Kg/kg		
Length Scale	0.1163 m	0.1163 m	0.0869 m
No. Inlet	6	6	6

3.1.2 The Outlet Air Conditions:

Table 3: Boundary conditions of the outlet

Length	Width	Type	Hydraulic diameter	No. of outlet
1.2 m	0.60 m	Pressure outlet	0.8 m	6

3.1.3 The Lighting:

The lights are treated as a warm surface supplying a uniform heat flux to the air estimated to be 2 W/m^2.

Table 4: Boundary conditions of the lighting unit

Length	Width	Type	Heat flux	No. of the lighting unit
1.2 m	0.60 m	Wall	2 W/m^2	32

3.1.4 The Walls:

Table 5 outlines the boundary conditions for the walls in the indoor swimming pool hall. The interior walls were divided into two, with the east and south sides set to a temperature of 20 ℃ during summer and winter. Similarly, the exterior walls were divided into two, with the north and west sides set to 25 ℃ during summer and -20 ℃ during winter.

The selection of these boundary conditions was essential to ensure accurate simulation results for the temperature distribution within the swimming pool hall. The temperatures set for the walls varied depending on the location and time of the year, allowing for a more realistic simulation that takes into account seasonal changes.

Table 5: Boundary conditions of the walls

Type	No. of wall	Conditions	Temperature	Location
Interior walls	2	summer	20 ℃	East and South Sides
		winter	20 ℃	
Exterior walls	2	summer	25 ℃	North and West Sides
		winter	-20 ℃	

3.1.5 The Pool:

The mass flow rate of water vapor was determined by the difference between the temperature of the air and the water and the relative humidity of the air.

Table 6: Boundary conditions of the pool

Length	Width	Hydraulic diameter	Type	Temperature	Specific humidity Kg/kg	Length scale	Mass flux Kg/m2.s
25 m	14 m	18 m	Mass flow inlet	29 ℃	0.0257	12.6 m	2.97×10^{-5} [2] [9]

4. Grid Independency Check

The grid independence check achieved through comparisons of the same configuration for different grid sizes of 3.5, 5.6, 6.9, and 10 Million. The comparison is made through-line plot shown in
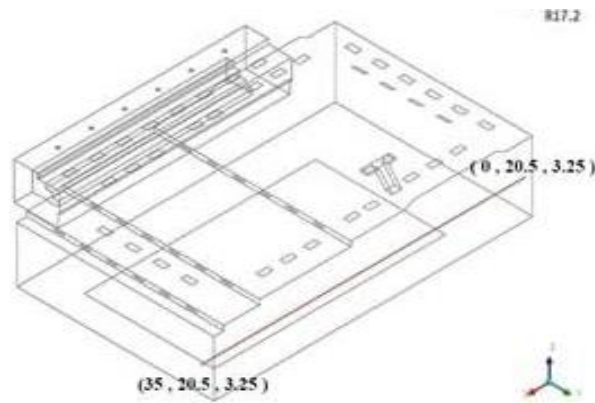
Figure 10: Line 1 configuration

4.1 Mesh quality

Recommendations by ANSYS low orthogonal quality or high skewness values are not recommended [11]. Table 7 shows the skewness mesh metrics spectrum, with corresponding ratings ranging from excellent to unacceptable. This table provides a guideline for evaluating the quality of the mesh in the simulation, with lower skewness values indicating a higher quality mesh.

Table 7: Skewness mesh metrics spectrum [12]

Excellent	Very Good	Good	Acceptable	Bad	Unacceptable
0-0.25	0.25-0.50	0.50-0.80	0.80-0.94	0.95-0.97	0.98-1.00

Table 8 presents the orthogonal quality mesh metrics spectrum, The spectrum ranges from "Unacceptable" to "Excellent," with corresponding values of 0-0.001, 0.001-0.14, 0.15-0.25, 0.20-0.69, 0.70-0.95, and 0.95-1. Values falling within the "Unacceptable" to "Bad" range indicate poor mesh quality, while values in the "Acceptable" to "Very Good" range indicate satisfactory to good mesh quality. Values falling in the "Excellent" range represent the best quality mesh. This spectrum is used to evaluate the quality of the mesh used in the numerical simulations and to identify potential issues related to the mesh.

Table 8: Orthogonal quality mesh metrics spectrum [11]

Unacceptable	Bad	Acceptable	Good	Very Good	Excellent
0-0.001	0.001-0.14	0.15-0.25	0.20-0.69	0.70-0.95	0.95-1

Table 9: Orthogonal quality and skewness values for grid sizes

Mesh Quality Metrics	Grid sizes			
	3.5 Million	5.6 Million	6.9 Million	10 Million
Orthogonal Quality	0.34	0.37	0.36	0.39
Skewness	0.65	0.62	0.63	0.60

The effect of different mesh sizes on temperature, relative humidity, and velocity profiles was illustrated as shown in Figure 11: Temperature profiles at line **1**, Figure 12: Relative humidity profiles at line 1, and Figure 13: Velocity profiles at line 1 depict the temperature, Velocity, and relative humidity distribution along line 1.
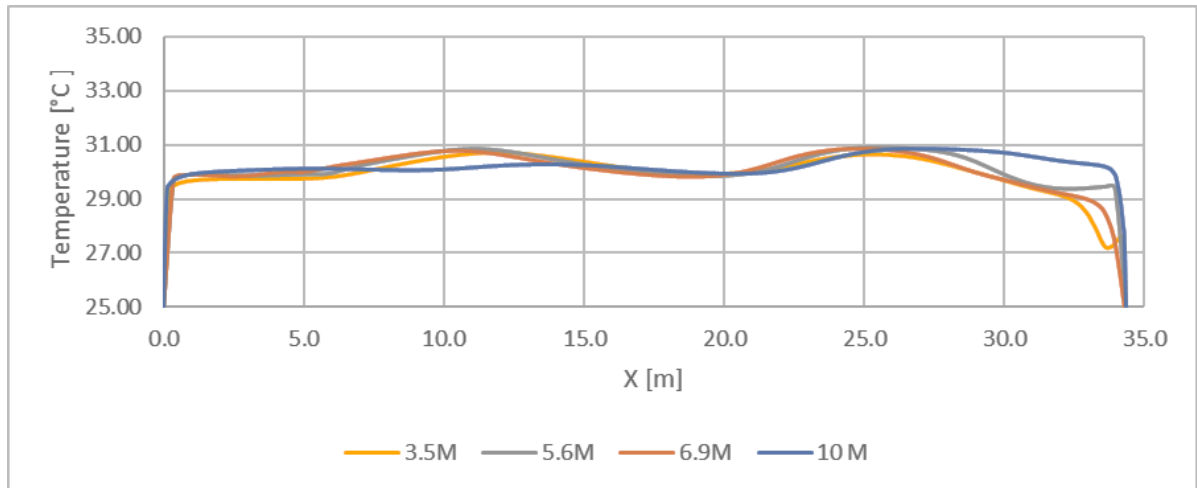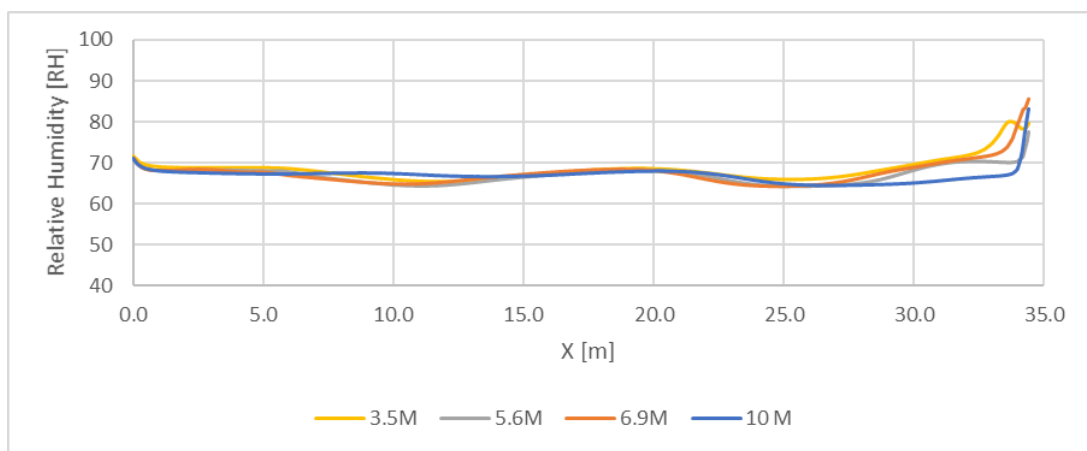
Figure 11: Temperature profiles at line 1

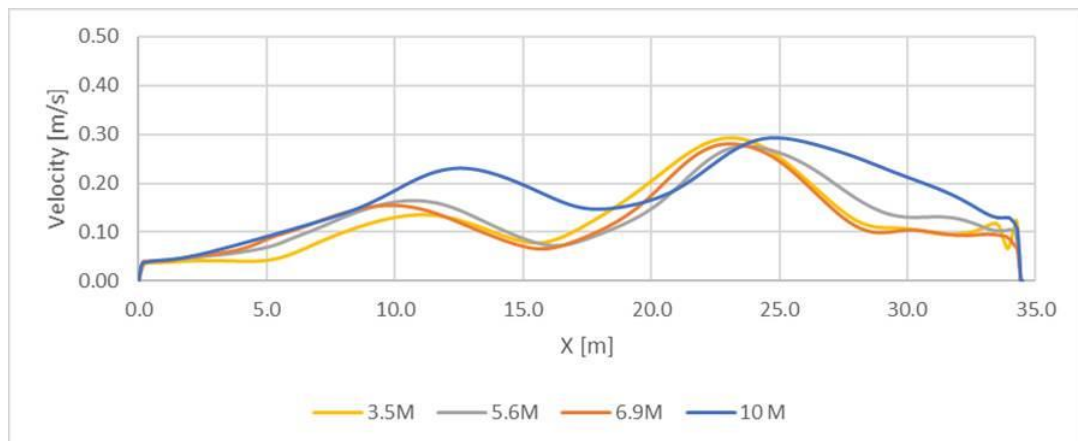**Figure 12: Relative humidity profiles at line 1**

Figure 13: Velocity profiles at line 1

The results using the four meshes show that the difference is insignificant but, the computing time of the fine mesh is 2 times slower. Therefore, the 5.6 Million mesh used for all simulations.

5. Validation Work

The Present comparisons between the numerical results using ANSYS Fluent Software to those previously published experimental and numerical results obtained by different researchers in the field using OpenFOAM software. By comparing velocity and Relative Humidity profiles at four lines in X-axis shown in

Figure **14**, and the cartesian coordinates of the line 1,2,3 and 4 shown in Error! Reference source not found.**.**
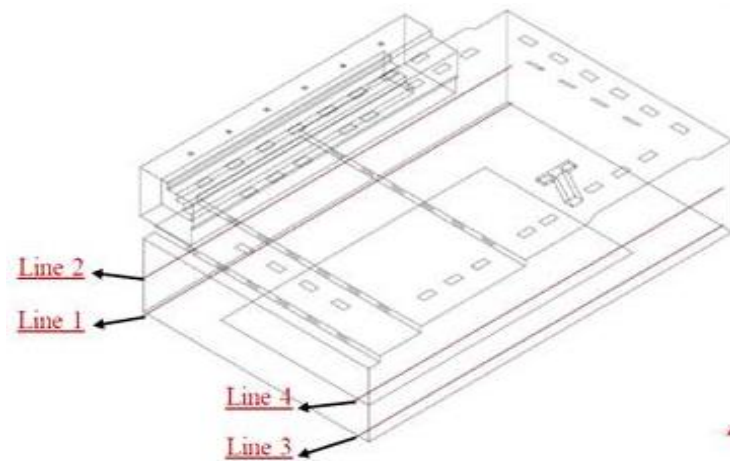
Figure 14: Lines 1,2,3 and 4 configurations

Table 10: Cartesian coordinates of the lines 1,2,3 and 4

	1st point			2nd point			Note
	X	Y	Z	X	Y	Z	
Line 1	0	0.5	0.2	35	0.5	0.2	
Line 2	0	0.5	3.25	35	0.5	3.25	In the same plane with line 1
Line 3	0	20.5	0.2	35	20.5	0.2	
Line 4	0	20.5	3.25	35	20.5	3.25	In the same plane with line 3
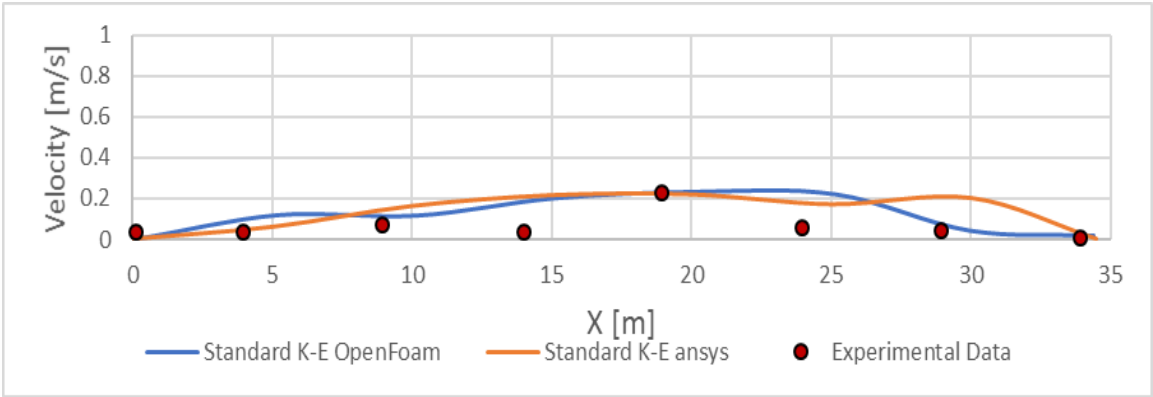
Figure 15: Velocity profiles at line 1
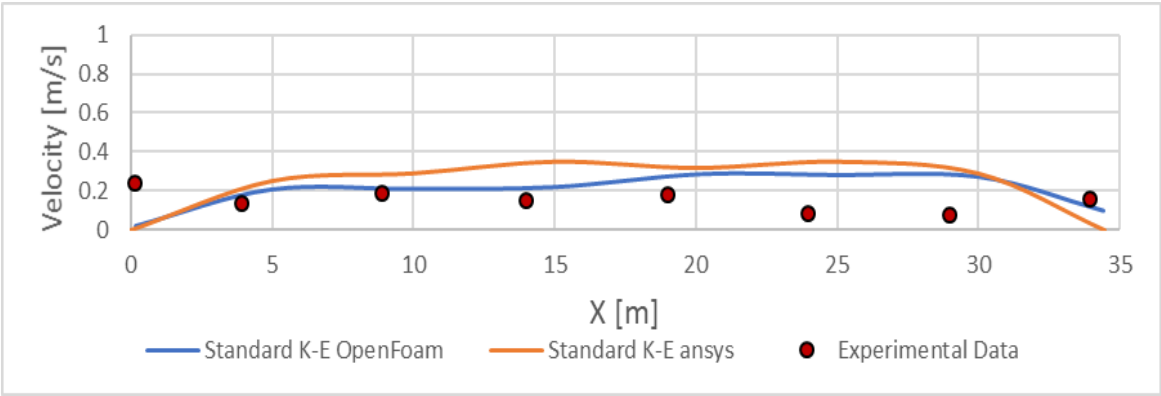
Figure 16: Velocity profiles at line 2
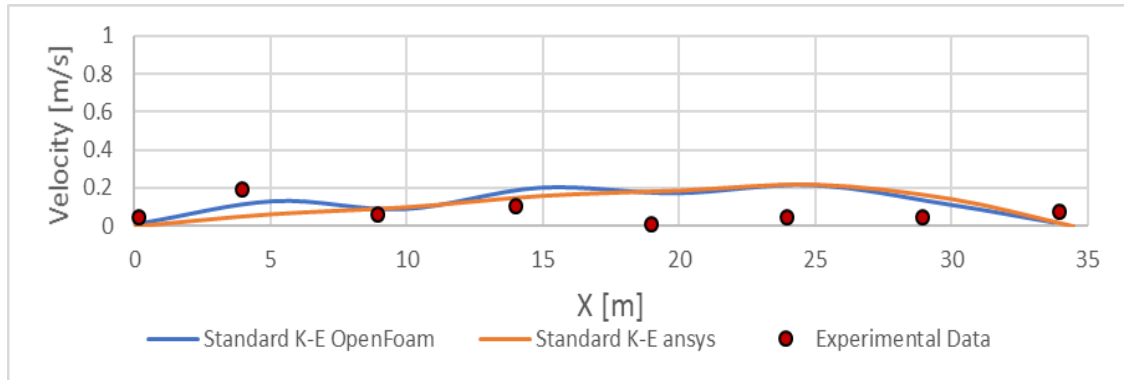
Figure 17: Velocity profiles at line 3
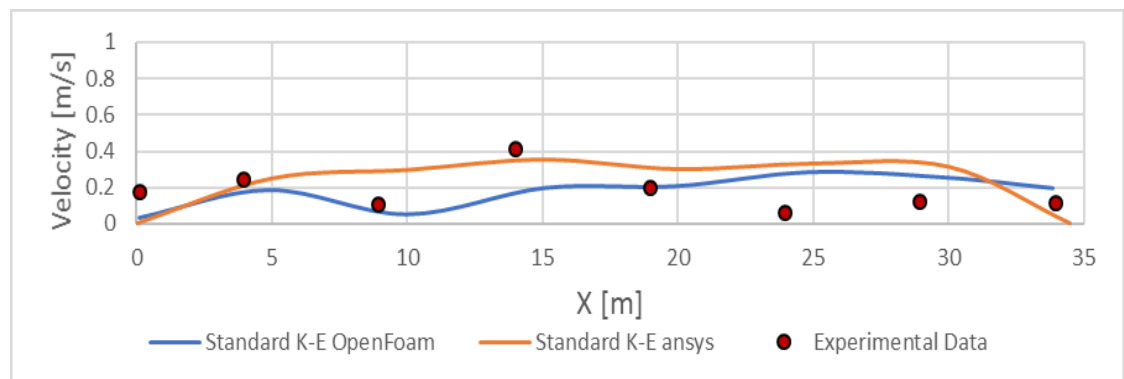
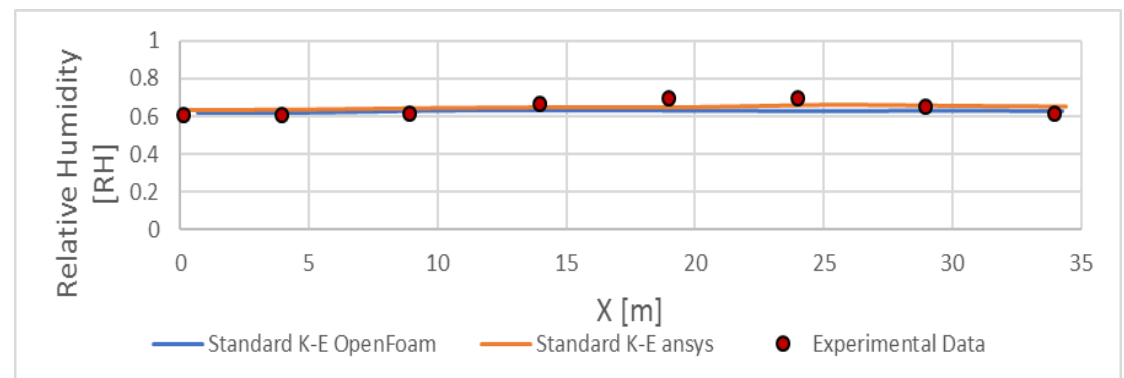**Figure 18: Velocity profiles at line 4**

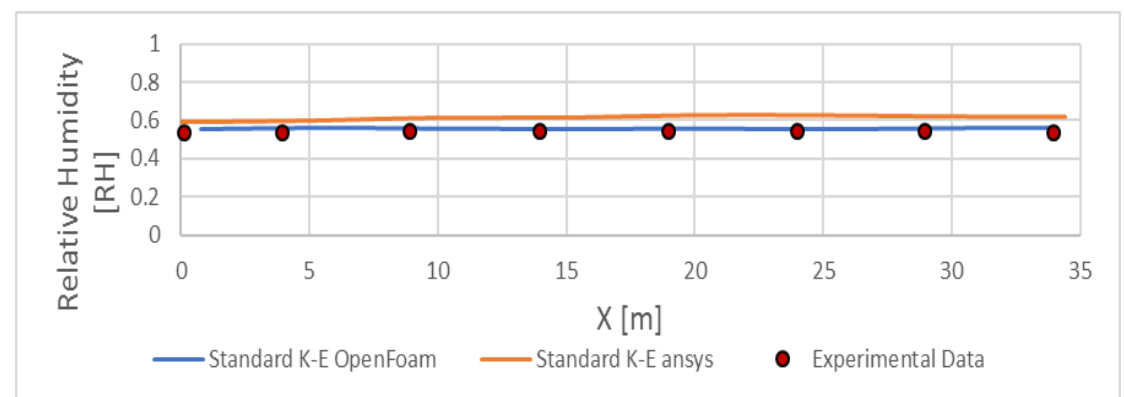**Figure 19: Relative humidity profiles at line 1**

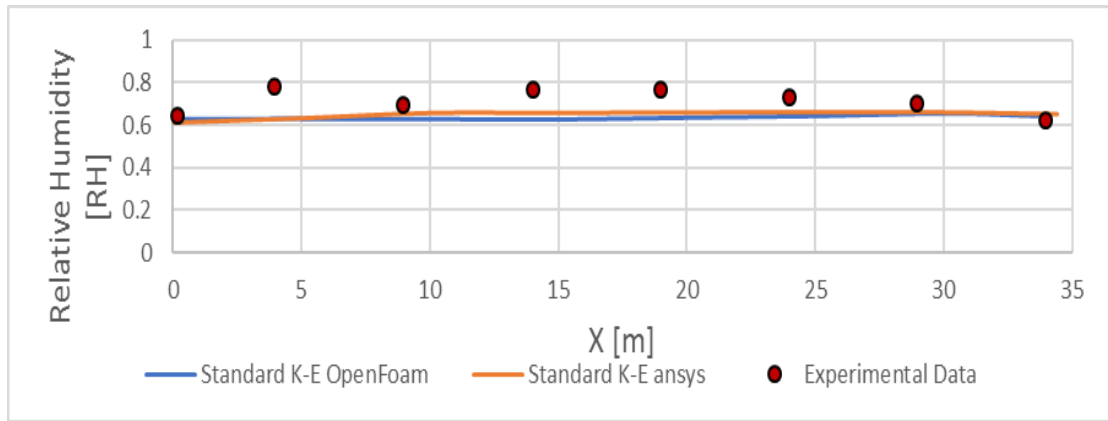**Figure 20: Relative humidity profiles at line 2**

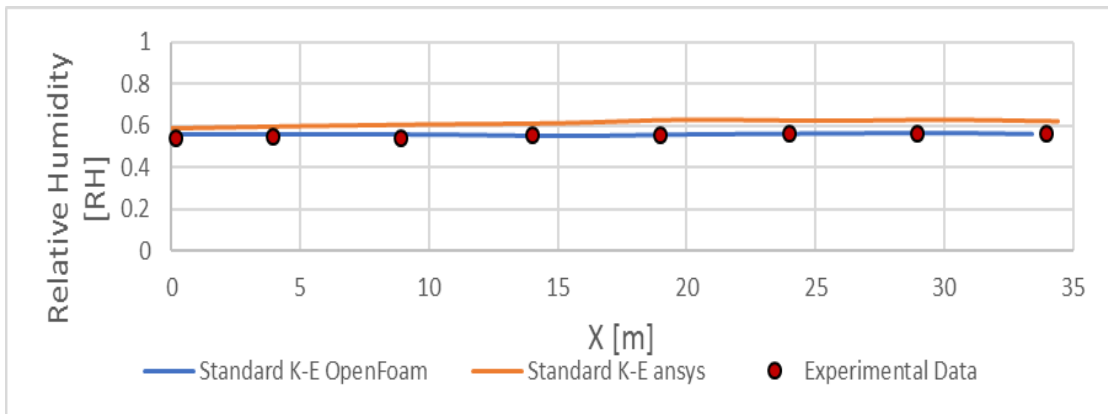**Figure 21: Relative humidity profiles at line 3**
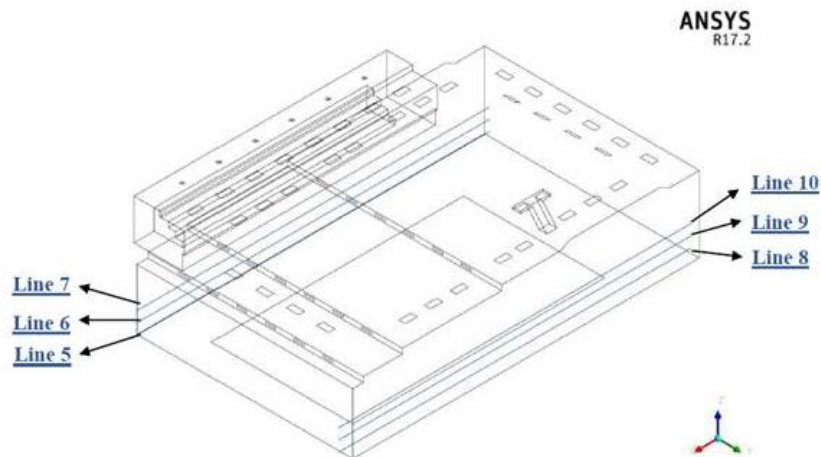

Figure 22: Relative humidity profiles at line 4

Figure 23: Line 5,6,7,8,9 and 10 configurations

Table 11: Cartesian coordinates of the lines 5,6,7,8,9 and 10

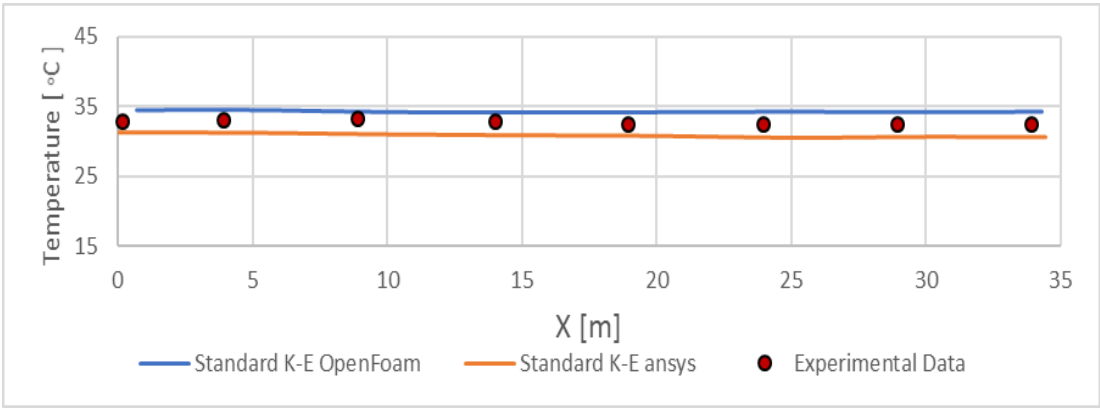| Line	1st point			2nd point			Note
	X	Y	Z	X	Y	Z	
5	0	0.5	0.45	35	0.5	0.45	
6	0	0.5	1.5	35	0.5	1.5	Lines 5,6 and 7 located in the same plane
7	0	0.5	2.55	35	0.5	2.55	
8	0	20.5	0.45	35	20.5	0.45	
9	0	20.5	1.5	35	20.5	1.5	Lines 8,9 and 10 located in the same plane
10	0	20.5	2.55	35	20.5	2.55	

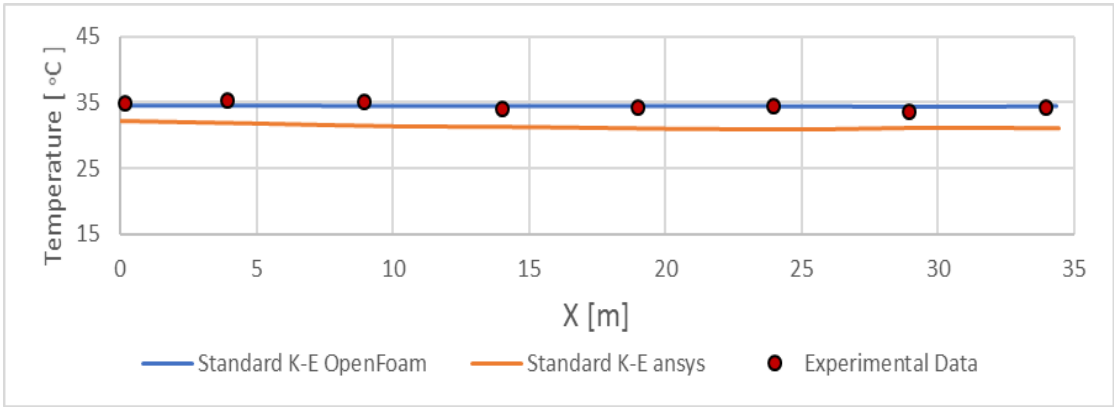**Figure 24: Temperature profiles at line 5**

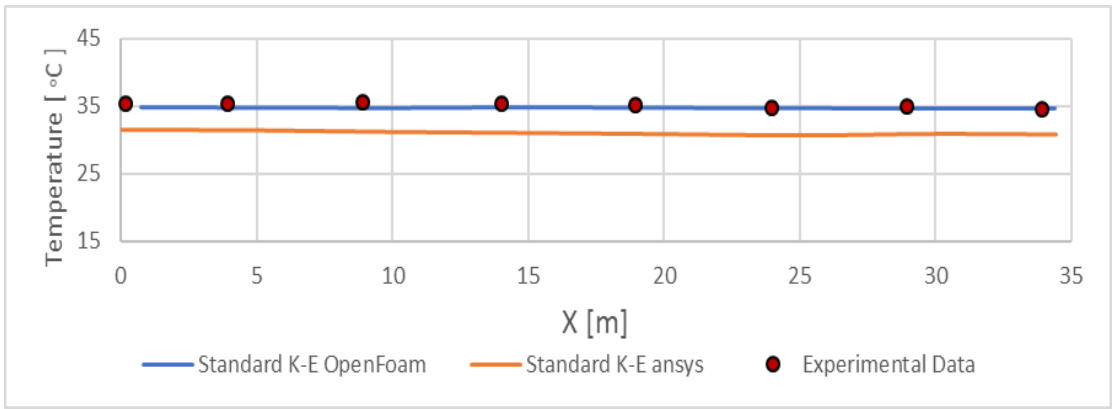**Figure 25: Temperature profiles at line 6**
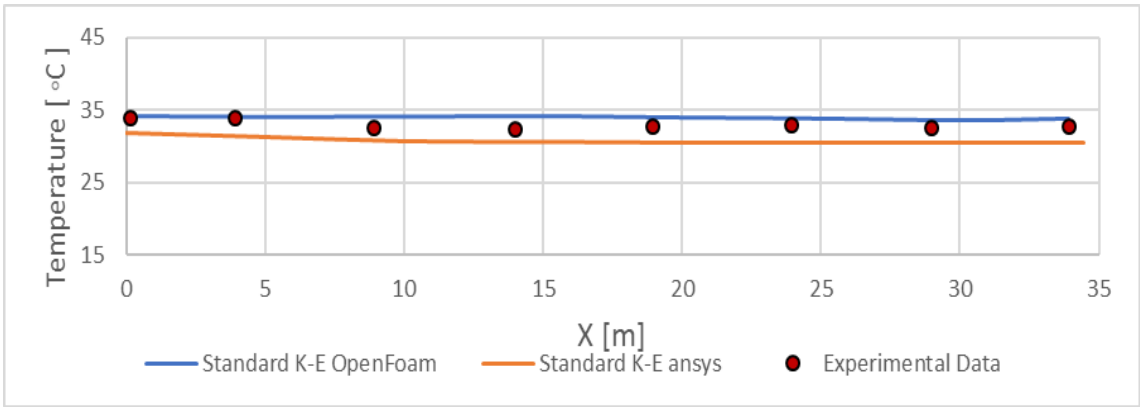

Figure 26: Temperature profiles at line 7

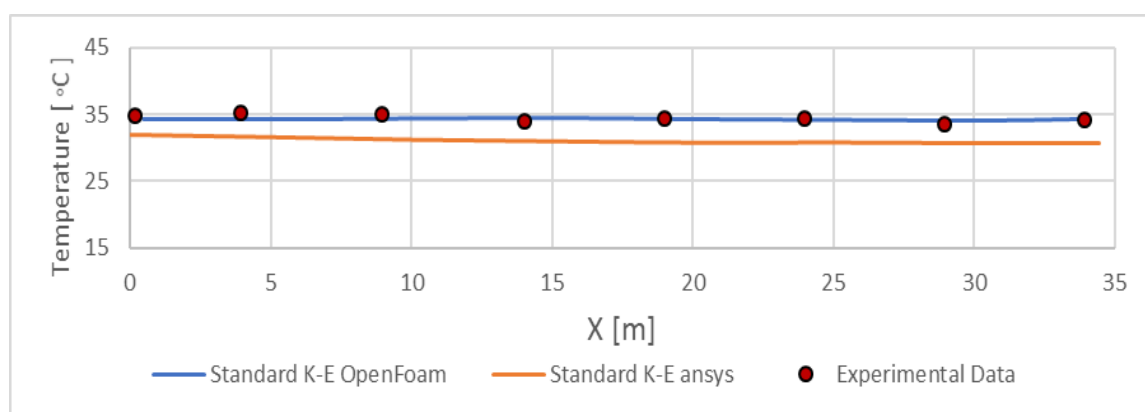**Figure 27: Temperature profiles at line 8**

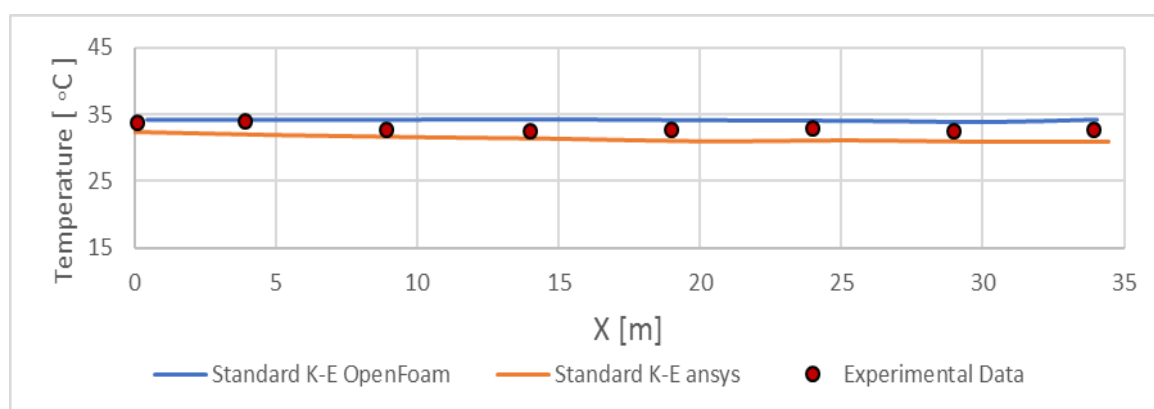**Figure 28: Temperature profiles at line 9**

Figure 29: Temperature profiles at line 10

6. Discussion

The present study compared the results obtained from two CFD software packages, ANSYS Fluent, and OpenFOAM, and found that ANSYS Fluent provided better predictions in several aspects. The error between the Standard K-ε Ansys and experimental data was within an acceptable range, indicating that the simulation was reasonably accurate. One important difference between the two software packages was the boundary condition of water vapor that evaporated from the pool. In OpenFOAM simulation, it was defined as an air layer with a relative humidity of 100% at 29 ℃, whereas in the Ansys simulation, it was defended with a mass flow rate from the pool surface, as recommended by M. M. Shah [3]. This approach led to a better defense of the evaporate rate and improved the overall accuracy of the simulation.

Conclusion

This study developed and validated a numerical code for simulating the velocity, temperature, and relative humidity distributions of the air, as well as the surface temperature of the walls, ceiling, and floor in a public indoor swimming pool at Bishop's University in Sherbrooke, Quebec, Canada. The comparison between ANSYS Fluent and OpenFOAM software showed a good agreement between the results of the two packages, with ANSYS Fluent providing more accurate predictions in several aspects. The use of ANSYS Fluent can lead to an improved ventilation system in indoor swimming pools, which can provide a comfortable and hygienic environment for users.

Future Work:

Despite the significant contributions of this study to the understanding of air conditioning systems in indoor swimming pools, there are still several areas that require further investigation. One potential avenue for future work could be to explore the effect of different air curtain

designs and configurations on the performance of air conditioning systems. Another possible direction would be to investigate the impact of different ventilation and air conditioning supply locations on the temperature and moisture distribution inside the swimming pool hall. Moreover, incorporating the effect of human activity in the pool hall on the air conditioning system could be an interesting area for future research. Finally, the impact of the surrounding environment, such as outdoor temperature and humidity, on the performance of indoor swimming pool air conditioning systems warrants further investigation.

References

1. A. Limane, H. Fellouah and N. Gal, "Simulation of airflow with heat and mass transfer in an indoor swimming pool by OpenFOAM," International Journal of Heat and Mass Transfer, vol. 109, pp. 862-878, 2017.

2. M. M. Shah, "Methods for Calculation of Evaporation from Swimming Pools and Other Water Surfaces," in ASHRAE, 2014.

3. M. Abo Elazm and A. I. Shahata, "Numerical and Field Study of the Effect of Air Velocity and Evaporation Rate on Indoor Air Quality in Enclosed Swimming Pools," International Review of Mechanical Engineering (IREME), vol. 9, no. 1, p. 97, 2015.

4. M. Lebon, H. Fellouah and N. Galanis, "Numerical Analysis and Field Measurements of The Airflow Patterns and Thermal Comfort in An Indoor Swimming Pool: A Case Study," Energy Efficiency, vol. 10, no. 3, pp. 527-548, 2016.

5. S. R. Applied computational fluid dynamics and turbulence modeling, Cham: Springer, 2019.

6. A. W. D. Anil W. Date: Introduction to computational fluid dynamics, Cambridge: Cambridge Univ. Press, 2009.

7. F. M. White and I. C. , Viscous fluid flow, New York: McGraw-Hill, 2006.

8. A. J. M. J. E. &. M. J. E. Chorin, A Mathematical Introduction To Fluid Mechanics, New York: Springer-Verlag, 1990.

9. Y. Cengel, Heat and Mass Transfer: Fundamentals & Applications, New York: McGraw-Hill Higher Education, 2014.

10. J. Luis, I. Rodríguez, F. Javier and P. Álvarez, "A New Practical CFD-Based Methodology to Calculate The Evaporation Rate in Indoor Swimming Pools," Energy and Buildings, vol. 149, pp. 133-141, 2017.

11. ANSYS, ANSYS Fluent Theory Guide, 2011.